Electronic Properties of BaFe$_2$As$_2$ upon Doping and Pressure: The Prominent Role of the As p Orbitals

V. Balédent, F. Rullier-Albenque, D. Colson, J. m. Ablett, J.-P. Rueff

Electronic Properties of BaFe$_2$As$_2$ upon Doping and Pressure: The Prominent Role of the As p Orbitals

V. Balédent,[1,][*] F. Rullier-Albenque,[2] D. Colson,[2] J. M. Ablett,[3] and J.-P. Rueff[3,4]

[1]*Laboratoire de Physique des Solides, 91400 Orsay, France*
[2]*SPEC CEA l'Orme les merisiers, 91191 Gif-sur-Yvette Cedex, France*
[3]*Synchrotron SOLEIL, L'Orme des Merisiers, BP 48 Saint-Aubin, 91192 Gif-sur-Yvette Cedex, France*
[4]*Université Pierre et Marie Curie, LCPMR, CNRS UMR7619, 11 rue Pierre et Marie Curie, 75005 Paris, France*

Using high-resolution, lifetime removed, x-ray absorption spectroscopy at the As K edge, we evidence the strong sensitivity of the As electronic structure upon electron doping with Co or pressure change in BaFe$_2$As$_2$, at room temperature. Our results unravel the prominent role played by As-$4p$ orbitals in the electronic properties of the Fe pnictide superconductors. We propose a unique picture to describe the overall effect of both external parameter doping and pressure, resolving the apparent contradiction between angle-resolved photoemission spectroscopy, transport, and absorption results, with the As-p states as a key ingredient.

The layered iron-based pnictides (FeSC) have emerged recently as a new class of high temperature superconductors with intriguing properties, igniting a worldwide burst of interest. The FeSC consists of FeAs layers separated by pnictogen, chalcogen, or rare-earth oxide blocking layers. Soon after the first report of superconductivity in LaFeAsO [1] ($T_c = 26$ K), numerous other compounds with higher critical temperature were discovered, such as SmFeAsO ($T_c = 55$ K), offering a complete new set of materials for the study of unconventional superconducting state. Most of FeSC share the same generic phase diagram. The parent compound generally undergoes a spin density wave transition at low temperature almost concomitant to a tetragonal-to-orthorhombic structural transition. Upon doping or applying pressure, both structural and magnetic transitions progressively vanish while superconductivity settles in with a dome-shaped critical temperature as a function of doping or pressure. This phase diagram is somewhat reminiscent of that of the cuprates. But despite their apparent similarity—both are layered systems with the $3d$ electrons as a key ingredient—superconductivity and antiferromagnetism live in close proximity–FeSC appear to be significantly distinct. Among the major differences, a multiorbital description is necessary for Fe-based superconductors whereas cuprates are often considered as a single orbital problem. The parent compound of the cuprates is a strongly correlated Mott insulator whereas it is a weakly correlated semimetal for the FeSC [2]; thus, it cannot be described by the single-band Mott-Hubbard model. This evokes the possibility in the FeSC of a superconducting mechanism of unconventional nature and different from the cuprates.

A crucial issue, yet to be fully understood, is the respective effect of doping and pressure on the electronic structure of the Fe-As active planar layer. To that purpose,

the BaFe$_2$As$_2$ family has been extensively studied. Indeed, it offers the possibility to induce superconductivity by isovalent (Ru on Fe sites) or nonisovalent (K onto Ba site or Co, Ni, Rh, and Pd onto the Fe sites) substitution or by applying hydrostatic pressure. If the equivalence of pressure and doping at the structural level has been firmly established [3], their respective influence on the electronic properties is far from being settled. Worryingly enough, the experimental results derived from the different probes of the electronic structure provide contradicting conclusions. On the one hand, photoemission measurements indicate a filling of the Fe-$3d$ bands upon doping. In this rigid band model picture, the Co supplementary electron adds to the existing bands, leading to a chemical potential shift [4–6]. Its direct consequence would be the increase in size of the Fermi surface, explaining the transport measurement results [7,8]. On the other hand, absorption spectroscopy at the Fe K edge reports no sign of such a shift, neither upon Co doping [9] nor under pressure [10]. Moreover theoretically, density-functional theory calculations found the extra d electron to be located on the substituted site [11] in agreement with Fe [12] and Co [13] $L_{2,3}$ edge absorption experiments. This striking contradiction is further reinforced by the sensitivity of the absorption to the chemical potential shift reported in fluorine-doped LaFeAsO [14]. In these works, however, the role of As has been greatly overlooked. Here, we report a doping and pressure study of BaFe$_2$As$_2$ using hard x-ray absorption spectroscopy (XAS) at high resolution beyond the lifetime broadening effect with a focus on the As K edge. Our results shed new light on the effect of both control parameters on the electronic structure while revealing the prominent role played by the As p states, and more generally on the role played by the ligand in correlated materials.

Pure and Co-doped single crystals of $BaFe_2As_2$ were grown using the self-flux method as described in Ref. [7]. The samples were extensively characterized by resistivity and SQUID measurements. The cobalt concentration has been determined within 0.5% accuracy by electron probe and confirmed by transport and thermodynamics properties. For the high-pressure experiment, a piece of $BaFe_2As_2$ (80 μm wide, 20 μm thick) was loaded in a membrane-driven diamond anvil cell using a Re gasket and silicon oil as a pressure transmitting medium. The pressure inside the diamond anvil cell was estimated using the ruby fluorescence technique, yielding a precision below 0.5 GPa [15]. XAS at the As K edge was performed on the GALAXIES beam line at the SOLEIL synchrotron [16]. The high-resolution spectra have been obtained in the partial fluorescence yield (PFY) mode at the As K_α emission line at 10.54 keV. We use a 1 m spherically bent Si(555) analyzer and an avalanche photodiode detector arranged in the Rowland circle geometry for measuring the emission spectra. The PFY spectra were recorded by monitoring the emission main line intensity as the incident energy was swept across the As K edge. Thanks to the second-order PFY process, the XAS K-edge spectra can be obtained with higher intrinsic resolution with respect to standard XAS partly free from the 1s lifetime broadening effect [17]. This sharpening effects is due the longer lifetime of the 2p core hole left in the $K\alpha$ emission final state with respect to the 1s core hole. All the spectra have been normalized to unity at high energy.

Figure 1(a) shows the doping dependence of the XAS spectra as a function of Co concentration at room temperature. The doping range covers the whole phase diagram from undoped to overdoped $Ba(Fe_{1-x}Co_x)_2As_2$ with $x = 20\%$. The difference with respect to the undoped sample is highlighted by the filled curves (here multiplied by a factor of 2 for the sake of visibility). The spectra show basically no change up to $x = 6\%$. Above this concentration, a sudden increase of the near-edge intensity occurs, marking a clear discontinuity in the doping evolution. The pressure dependence of the pure parent compound is represented in Fig. 1(b), together with the differences with respect to ambient pressure (multiplied by a factor of 2). The pressure varies from ambient pressure to 10 GPa, thus covering the whole phase diagram from the normal state to the superconducting region and further beyond. All the low-pressure spectra (not shown here) up to 0.9 GPa are identical to that measured at ambient pressure within the instrumental resolution. A clear discontinuity occurs at 1 GPa, reminiscent of that observed in the doping dependence at $x = 0.6\%$. Above 1 GPa, we observed a strong modification of the near-edge shape similar to the one observed upon doping that cannot be ascribed to a rigid shift of the ambient pressure spectrum, as shown in Fig. 2.

We now focus on the difference spectra in order to analyze more quantitatively the spectral change as a function of
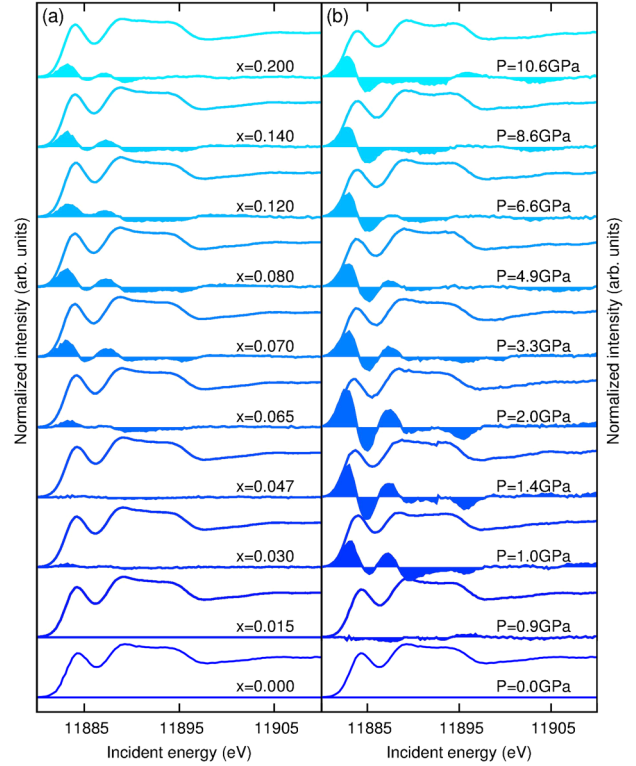

FIG. 1 (color online). Left: Absorption spectra at the As K edge in $Ba(Fe_{1-x}Co_x)_2As_2$ measured in the PFY mode for different concentrations of Co at room temperature. The spectral differences with respect to the parent (undoped) compound are represented by the filled curves. The differences are multiplied by a factor of 2 for the sake of visibility. Right: Absorption spectra evolution as a function of pressure for the undoped compound and differences with respect to the ambient pressure data (filled curves), multiplied by a factor of 2.

doping or pressure in the proximity of the Fermi energy around 11 882 eV. The difference spectra were fitted by the sum of two Gaussian functions centered at 11 882.8 and 11 887.5 eV with a null background [18]. The fit results are represented in Fig. 3. The intensities are reported for both pressure (black circles) and doping (red triangles) dependence on the left-side of Fig. 3 for the 11 882.8 eV feature only; the 11 887.5 eV peak exhibits exactly the same doping and pressure evolution, showing that it pertains to the same electronic states.

As observed from the crude inspection of the data, our analysis confirms the discontinuous behavior of the doping or pressure dependence with a jump in the spectral changes at around $x_c = 6.5\%$ and $P_c = 1$ GPa, respectively. Incidentally, the value of x_c coincides with the maximum of the superconducting critical temperature. This also corresponds to the Co doping at which the evolution of the electron concentration suddenly inverts as expected for a rigid band model [8], a behavior sometimes referred to as a Lifshitz transition [20,21] and suggesting a sudden reorganization of the electronic structure near this concentration.
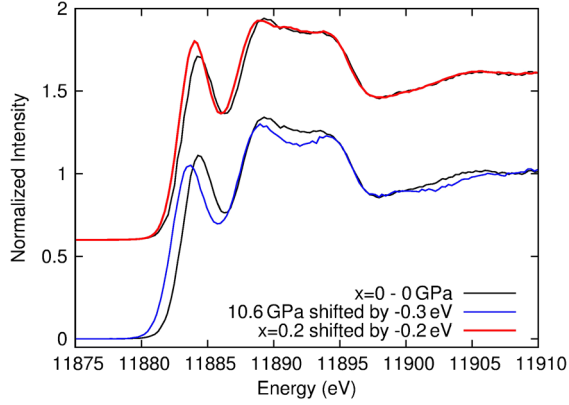
FIG. 2 (color online).   Comparison of the As K-edge spectra in the undoped compound at ambient condition (black line) with the spectra measured in the doped (red line) compound and under pressure (blue line) shifted in energy. The rigid energy shift cannot reproduce the spectral changes.

It is tempting to look for a common mechanism underlying the pressure and doping dependences since both show a similar behavior. To that end, we have converted the Co concentrations and pressures into Fe-As interatomic distances using the data of Refs. [12,19]. The results are displayed in Fig. 3(c). The discontinuity is found at a Fe-As distance of 2.39 Å independently of the control parameter, suggesting a close link between the electronic structure changes and the Fe-As distance, and thus of Fe-3d and As-4p hybridization.

The crucial role of Fe-As hybridization for the electronic structure of the Fe pnictides has been reported previously [13,22,23]. The application of a hydrostatic pressure decreasing the Fe-As distance is expected to increase the overlap between Fe and As orbitals, reinforcing their hybridization. To further investigate the effects of hybridization, we performed numerical simulations of the As K edge in BaFe$_2$As$_2$ using the FDMNES code [24]. We used a cluster radius of 17 Å to reach full convergence. The structural parameters in the space group ($I4/mmm$) at ambient conditions were taken from Ref. [25]. The effects of pressure were taken into account by contracting the lattice parameters according to the diffraction data [25]. The main results are shown in Fig. 4. The simulated XAS spectra (top part in Fig. 4) show a fair agreement with the experimental ones, especially in the low energy region, the most sensitive to Fe-As hybridization. Importantly, the calculations are able to correctly reproduce the electronic changes with pressure as can be inferred from the spectral differences between 0 and 7 GPa. It is reasonable then to pay further attention to the density of states (DOS) extracted from the FDMNES calculations as an insight into the electronic changes under pressure. For the sake of clarity in Fig. 4, we restrict ourselves to the projected DOS for the Fe-3d and As-4p orbitals calculated at ambient pressure and 7 GPa, well above the transition pressure P_c. Notice that in our experimental configuration, the incident
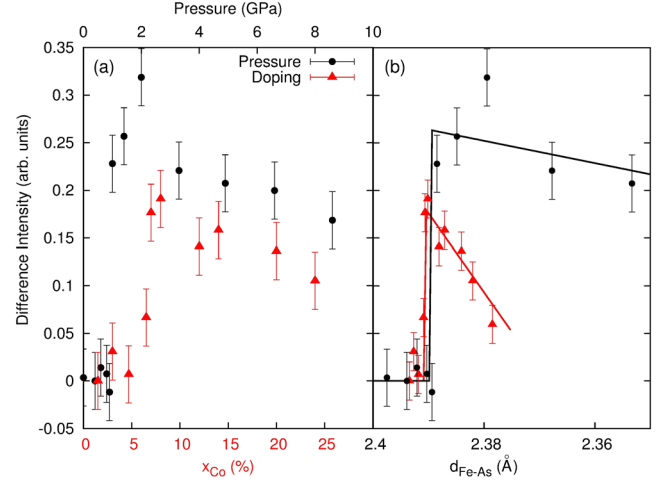

FIG. 3 (color online).   Left: Evolution of the 11 882.8 eV peak intensity in the difference spectra (cf. Fig. 1) from the fit analysis as a function of doping (red triangles, lower axis) and pressure (black circles, upper axis); see text for details. Right: Same data as in the left-hand panel as a function of the Fe-As interatomic distance; we used Refs. [12,19] for converting pressure and doping to interatomic distance. Lines are guides for the eyes.

beam was set perpendicular to the ab plane, so that the XAS measurements are not sensitive to the p_z orbital of As. In accordance with the measurement geometry, only the $p_x + p_y$ projected DOS is represented for As. The calculated DOS confirm the strong hybridization between the As-p and Fe-3d states. As illustrated in the bottom part of Fig. 4, the effect of pressure on the As-4p projected DOS mainly affects the occupied states below the Fermi level (around 11 882 eV) with a shift of ~0.5 eV toward the low energies when pressure is increased. The unoccupied states (around 11 884 eV) are also slightly shifted to the same direction but to a lesser extent. The direct consequence of this renormalization of the carrier density is the increase of the number of occupied states below the Fermi energy with an As character. Because of the reinforced hybridization induced by the Fe-As distance shortening, a similar behavior is observed for the Fe-3d orbitals. With respect to the chemical potential, the DOS of Fe-3d undergoes a global shift toward the low energies simultaneously to the As-4p states. It is worth noting that, according to the simulation, the As-4p orbitals seem to hybridize more strongly with the d_z^2 and d_{xy} Fe orbitals that show the strongest effects.

Our results, together with the previous studies at the Fe K edge [9,10], give new insight on the respective roles of As-p and Fe-d orbitals. First, our results demonstrate the prominent role of the As p orbitals as the active electrons to pressure changes, and equivalently to doping, since both control parameters were shown to act similarly. This picture agrees with the theoretical predictions that the doped electrons are preferentially localized onto the As sites rather than the Fe sites. Second, our picture can reconcile XAS with angle-resolved photoemission spectroscopy
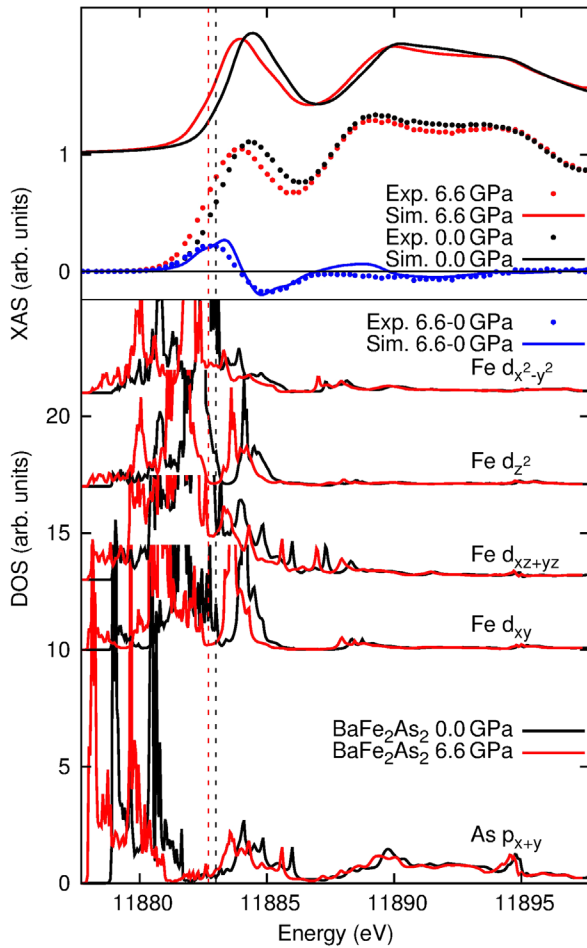
FIG. 4 (color online). Top: As-K XAS experimental (dots) and simulated (lines) spectra using the FDMNES code at 0 (black) and 6.6 (red) GPa; the position of the Fermi energy at 0 and 6.6 GPa is indicated by the dashed lines. The experimental differences (blue dots) agrees well with the simulated XAS spectral difference at the same pressures (blue line). Bottom: Projected density of states (solid lines) of the As-$4p$ and Fe-$3d$ orbitals for the undoped $BaFe_2As_2$ compound at ambient pressure (black) and 7 GPa (red).

(ARPES) and transport measurements. The photoemission experiments of Ref. [4] show an increase of the bandwidth of the Fe-$3d$ band upon Co doping. This behavior is interpreted in a rigid band model where the doping electrons are added to the Fe-$3d$ band, resulting in an increase of the chemical potential. We propose here that the doping electron remains on the Co site as long as the Fe-As distance exceeds the value of 3.9 Å, that is, for concentration lower than 6%. For higher concentration, the Fe-As distance decrease enhances the hybridization and enables the electron to delocalize from Co-$3d$ to As-$4p$ orbitals, forming free carriers in the conduction band. Because the electronic changes mainly affect the As-$4p$ orbitals, it also explains why the Fe K edge spectra remain unaltered in the whole pressure and doping phase diagram as previously reported [10]. Furthermore, our finding remains consistent

with the growth of the Fermi surface upon doping as exhibited by ARPES results and transport measurements. In a very similar way, pressure has no effect until a Fe-As distance of 3.9 Å is reached, around 1 GPa. Below this distance, hybridization is strong enough to enable the redistribution of the charge between Fe and As orbitals resulting in strong changes in the As electronic structure. Note that this crucial role of the ligand is not limited to $BaFe_2As_2$ and has been identified in many other correlated materials. In high temperature superconducting cuprates especially, there are growing indications from both theory [26] and experiment [27–29] that oxygen orbitals play a major role in the unconventional physics of copper oxides.

In conclusion, we have studied the electronic properties of the $BaFe_2As_2$ pnictide superconductors as function of pressure and Co doping using high-resolution x-ray absorption spectroscopy. The results demonstrate that Co doping and pressure have similar effects on the $BaFe_2As_2$ electronic structure due to the shortening of the Fe-As distance and the increase of Fe-As hybridization. Unexpectedly, this mostly alters the As-$4p$ states leading to a shift towards lower energy while Fe-$3d$ states undergo the same shift because of the growing hybridization strength. Our interpretation reconciles ARPES and transport measurements with absorption spectroscopy. This sheds new light on the prominent role of As for the understanding of the properties of the Fe superconductors.

*Corresponding author.
victor.baledent@u-psud.fr

[1] Y. Kamihara, H. Hiramatsu, M. Hirano, R. Kawamura, H. Yanagi, T. Kamiya, and H. Hosono, J. Am. Chem. Soc. **128**, 10012 (2006).

[2] W. L. Yang, A. P. Sorini, C.-C. Chen, B. Moritz, W.-S. Lee, F. Vernay, P. Olalde-Velasco, J. D. Denlinger, B. Delley, J.-H. Chu, J. G. Analytis, I. R. Fisher, Z. A. Ren, J. Yang, W. Lu, Z. X. Zhao, J. van den Brink, Z. Hussain, Z.-X. Shen, and T. P. Devereaux, Phys. Rev. B **80**, 014508 (2009).

[3] S. A. J. Kimber, A. Kreyssig, Y.-Z. Zhang, H. O. Jeschke, R. Valenti, F. Yokaichiya, E. Colombier, J. Yan, T. C. Hansen, T. Chatterji, R. J. McQueeney, P. C. Canfield, A. I. Goldman, and D. N. Argyriou, Nat. Mater. **8**, 471 (2009).

[4] V. Brouet, M. Marsi, B. Mansart, A. Nicolaou, A. Taleb-Ibrahim, P. LeFevre, F. Bertran, F. Rullier-Albenque, A. Forget, and D. Colson, Phys. Rev. B **80**, 165115 (2009).

[5] M. Neupane, P. Richard, Y.-M. Xu, K. Nakayama, T. Sato, T. Takahashi, A. V. Federov, G. Xu, X. Dai, Z. Fang, Z. Wang, G.-F. Chen, N.-L. Wang, H.-H. Wen, and H. Ding, Phys. Rev. B **83**, 094522 (2011).

[6] J. McLeod and A. Buling, J. Phys. Condens. Matter **24**, 215501 (2012).

[7] F. Rullier-Albenque, D. Colson, A. Forget, and H. Alloul, Phys. Rev. Lett. **103**, 057001 (2009).

[8] L. Fang, H. Luo, P. Cheng, Z. Wang, Y. Jia, G. Mu, B. Shen, I. I. Mazin, L. Shan, C. Ren, and H.-H. Wen, Phys. Rev. B **80**, 140508 (2009).

[9] E. Bittar, C. Adriano, and T. Garitezi, Phys. Rev. Lett. **107**, 267402 (2011).

[10] V. Balédent, F. Rullier-Albenque, D. Colson, G. Monaco, and J. P. Rueff, Phys. Rev. B **86**, 235123 (2012).

[11] H. Wadati, I. Elfimov, and G. A. Sawatzky, Phys. Rev. Lett. **105**, 157004 (2010).

[12] M. Merz, P. Schweiss, and P. Nagel, arXiv:1306.4222v1.

[13] M. Merz, F. Eilers, T. Wolf, and P. Nagel, Phys. Rev. B **86**, 104503 (2012).

[14] T. Kroll, S. Bonhommeau, T. Kachel, H. A. Dürr, J. Werner, G. Behr, A. Koitzsch, R. Hübel, S. Leger, R. Schönfelder, A. K. Ariffin, R. Manzke, F. M. F. de Groot, J. Fink, H. Eschrig, B. Büchner, and M. Knupfer, Phys. Rev. B **78**, 220502 (2008).

[15] H. Mao, J. Xu, and P. Bell, J. Geophys. Res. **91**, 4673 (1986).

[16] J.-P. Rueff, J. M. Ablett, D. Céolin, D. Prieur, T. Moreno, V. Balédent, B. Lassalle, J. E. Rault, M. Simon, and A. Shukla, J. Synchrotron Radiat. **22**, 175 (2015).

[17] F. M. F. de Groot, Chem. Rev. **101**, 1779 (2001).

[18] See Supplemental Material at http://link.aps.org/supplemental/10.1103/PhysRevLett.114.177001 for details of the fitting procedure.

[19] E. Granado, L. Mendonça-Ferreira, F. Garcia, G. de M. Azevedo, G. Fabbris, E. M. Bittar, C. Adriano, T. M. Garitezi, P. F. S. Rosa, L. F. Bufaiçal, M. A. Avila, H. P. Terashita, and P. G. Pagliuso, Phys. Rev. B **83**, 184508 (2011).

[20] E. D. Mun, S. L. Bud'ko, N. Ni, A. N. Thaler, and P. C. Canfield, Phys. Rev. B **80**, 054517 (2009).

[21] C. Liu, T. Kondo, and R. Fernandes, Nat. Phys. **6**, 419 (2010).

[22] C. Parks Cheney, F. Bondino, T. A. Callcott, P. Vilmercati, D. Ederer, E. Magnano, M. Malvestuto, F. Parmigiani, A. S. Sefat, M. A. McGuire, R. Jin, B. C. Sales, D. Mandrus, D. J. Singh, J. W. Freeland, and N. Mannella, Phys. Rev. B **81**, 104518 (2010).

[23] I. Nekrasov, Z. Pchelkina, and M. Sadovskii, JETP Lett. **88**, 144 (2008).

[24] O. Bunau and Y. Joly, J. Phys. Condens. Matter **21**, 345501 (2009).

[25] R. Mittal, S. K. Mishra, S. L. Chaplot, S. V. Ovsyannikov, E. Greenberg, D. M. Trots, L. Dubrovinsky, Y. Su, T. Brueckel, S. Matsuishi, H. Hosono, and G. Garbarino, Phys. Rev. B **83**, 054503 (2011).

[26] K. B. Efetov, H. Meier, and C. Pépin, Nat. Phys. **9**, 442 (2013).

[27] M. J. Lawler, K. Fujita, J. Lee, A. R. Schmidt, Y. Kohsaka, C. K. Kim, H. Eisaki, S. Uchida, J. C. Davis, J. P. Sethna, and E.-A. Kim, Nature (London) **466**, 347 (2010).

[28] S. De Almeida-Didry, Y. Sidis, V. Balédent, F. Giovannelli, I. Monot-Laffez, and P. Bourges, Phys. Rev. B **86**, 020504 (2012).

[29] E. Blackburn, J. Chang, M. Hücker, A. Holmes, N. Christensen, R. Liang, D. Bonn, W. Hardy, U. Rütt, O. Gutowski, M. Zimmermann, E. Forgan, and S. Hayden, Phys. Rev. Lett. **110**, 137004 (2013).